Progress In Electromagnetics Research Letters, Vol. 76, 1–6, 2018

Compact Microstrip Rotman Lens Using Chebyshev Impedance Transformers

Qiuyan Liang[1, *], Baohua Sun[1], Gaonan Zhou[1], and Jianfeng Li[2]

Abstract—A compact microstrip Rotman lens is proposed in this paper. The microstrip Rotman lens consists of a lens body and Chebyshev impedance transformers. The Chebyshev impedance transformers are used as beam ports, array ports and dummy ports. Compared to the traditional linear tapered transition, the Chebyshev impedance transformer is shorter, which leads to the size reduction and insertion loss improvement for the Rotman lens. An X-band 4×7 Rotman lens using Chebyshev impedance transformers is designed and fabricated. Compared to a traditional Rotman lens, the proposed Rotman lens shows a size reduction of about 56% and an insertion loss improvement at 10 GHz. The measured results demonstrate that better than 15 dB return loss throughout the bandwidth from 8 to 12 GHz is obtained.

1. INTRODUCTION

With the development of wireless communication systems, the antennas with beam scanning function have been highly desired [1, 2]. The Rotman lens is a passive beam former used in multi-beam antenna systems [3]. It can realize beam scanning function based on geometrical optic theory. Rotman lens has been widely used in many applications due to its many advantages such as multi-beam capability, true time delay characteristic and wide angular range beam scanning [4–6]. However, a traditional Rotman lens, which is composed of lens body and linear tapered transitions, tends to be large, which limits the integration in compact transceiver systems [7, 8]. There have been some solutions to reduce the size of multi-beam antenna systems. In [9], the lens body of Rotman lens is folded into two layers along its middle plane. In [10], the array ports and lens body are placed on different layers in multilayer substrate integrated waveguide (SIW) technology. Both methods in [9] and [10] reduce the dimensions of antenna systems compared to single-layer implementations. However, it is noted that the processing area, which is equal to the total multilayer areas, is not reduced. In addition, the multilayer process is complicated, which leads to the difficult fabrication process and high cost in massive productions.

In this paper, a compact single-layer microstrip Rotman lens is presented. The Rotman lens uses the Chebyshev impedance transformers as the beam ports, array ports and dummy ports. The Chebyshev impedance transformer has shorter length and less path loss, which leads to the size reduction and insertion loss improvement for the Rotman lens. An X-band prototype has been fabricated and measured. The proposed Rotman lens shows a size reduction of about 56% and an insertion loss improvement at the centre frequency compared with a traditional Rotman lens. The measured and simulated results are given and discussed in detail.

Received 7 March 2018, Accepted 30 April 2018, Scheduled 14 May 2018

* Corresponding author: Qiuyan Liang (qiuyanliang@stu.xidian.edu.cn).

[1] National Laboratory of Science and Technology on Antennas and Microwaves, Xidian University, Xi'an, Shaanxi 710071, China.

[2] KISEKI Auto (Zhejiang) Co. Ltd., Shuige Industrial Park, No. 291 Long-Qing Road, Lishui, Zhejiang 323000, China.

2. LENS DESIGN

The layout of the proposed Rotman lens is illustrated in Fig. 1(a). The proposed Rotman lens is printed on the top layer of a Rogers RO4350 substrate with relative permittivity of 3.66 and dielectric loss tangent of 0.004. The Rotman lens is composed of a lens body and Chebyshev impedance transformers [11]. The lens body is shaped of a focal arc and an inner lens contour. The lens contours and the locations of ports are designed based on the original Rotman lens design equations initially proposed by Rotman and Turner [3]. The Chebyshev impedance transformers constitute the beam ports, array ports and dummy ports of the Rotman lens. The Rotman lens has 4 beam ports B1–B4, 7 array ports A1–A7, and 6 dummy ports D1–D6. The beam ports are located along the focal arc to decide the beam directions. The array ports are located along the inner lens contour to achieve the corresponding path length differences. The dummy ports are located at two sides of the lens body to absorb extra wave reflected from the array ports. The design parameters of the Rotman lens are list in Table 1.

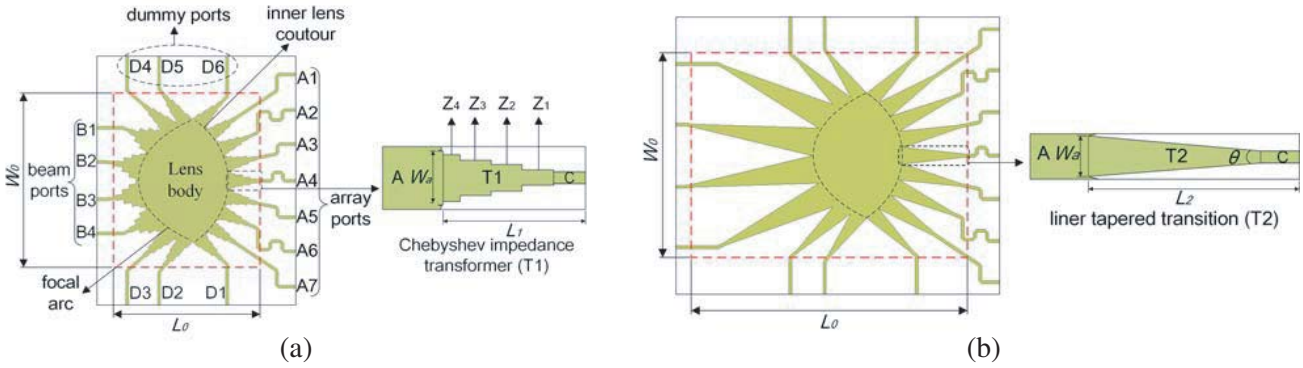

Figure 1. (a) Layout of proposed Rotman lens using Chebyshev impedance transformers. $W_a = 0.6\lambda_g$, $L_1 = 1.2\lambda_g$. (b) Layout of traditional Rotman lens using linear tapered transitions. $W_a = 0.6\lambda_g$, $L_2 = 2.3\lambda_g$.

Table 1. The design parameters of the Rotman lens.

Design frequency	Beam directions	Elements space	Substrate material	Substrate thickness
10 GHz	$\pm 10°$ and $\pm 30°$	18 mm	Rogers 4350	30 mil

As shown in Fig. 1(a), the Chebyshev impedance transformer, lensbody and feed line are represented by 'T1', 'A' and 'C', respectively. The lens body and feed line can be matched well through the Chebyshev impedance transformer. The Chebyshev impedance transformer consists of multi-section transmission lines with different characteristic impedances. Given the port aperture width W, the aperture impedance Z can be calculated by Eq. (1) [11]. Given the aperture impedance Z and the characteristic impedance of the feed line, the characteristic impedances of multi-section transmission lines can be calculated based on the small reflection theory [11]. The detailed design parameters of the Chebyshev impedance transformers are list in Table 2. (Because the Rotman lens is symmetrical, only the parameters for half of all ports are list).

$$Z = \begin{cases} \dfrac{60}{\sqrt{\varepsilon_e}} \ln\left(\dfrac{8d}{W} + \dfrac{W}{4d}\right) & \text{for } W/d \le 1 \\ \dfrac{120\pi}{\sqrt{\varepsilon_e}} \left[W/d + 1.393 + 0.667 \ln(W/d + 1.444)\right] & \text{for } W/d \ge 1 \end{cases} \tag{1}$$

For comparison purposes, a traditional Rotman lens using linear tapered transitions is also shown in Fig. 1(b). The linear tapered transition (represented by 'T2') has flare angle θ. The Rotman lens with

Table 2. Design parameters of the Chebyshev impedance transformers.

Port	B1	B2	A1	A2	A3	A4	D1	D2	D3
W/λ_g	1	1	0.6	0.6	0.6	0.6	0.5	0.5	0.5
N	3	3	4	4	4	4	3	3	3
$Z1\,(\Omega)$	40.1	40.1	45.9	45.9	45.9	45.9	43.4	43.4	43.4
$Z2\,(\Omega)$	30	30	33.3	33.3	33.3	33.3	28.6	28.6	28.6
$Z3\,(\Omega)$	10.9	10.9	20.9	20.9	20.9	20.9	18.8	18.8	18.8
$Z4\,(\Omega)$	-	-	15.2-	15.2-	15.2-	15.2-	-	-	-

Table 3. Performance comparison of Rotman lenses with different structures.

Rotman Lens	Band width of B1 (VSWR < 1.5)	Band width of B2 (VSWR < 1.5)	Insertion loss of B1 at 10 GHz	Insertion loss of B2 at 10 GHz	Area ($L_0 \times W_0$)
Traditional ($\theta = 12°$)	$> 40\%$	$> 40\%$	3.2 dB	2.6 dB	$9.6\lambda_g \times 7.2\lambda_g$
Traditional ($\theta = 24°$)	30.4%	$> 40\%$	2.6 dB	2.3 dB	$6.3\lambda_g \times 6.0\lambda_g$
Traditional ($\theta = 36°$)	16.1%	29.5%	2.4 dB	2.2 dB	$5.2\lambda_g \times 5.2\lambda_g$
Chebyshev	$> 40\%$	$> 40\%$	2.1 dB	1.7 dB	$5.0\lambda_g \times 6.1\lambda_g$

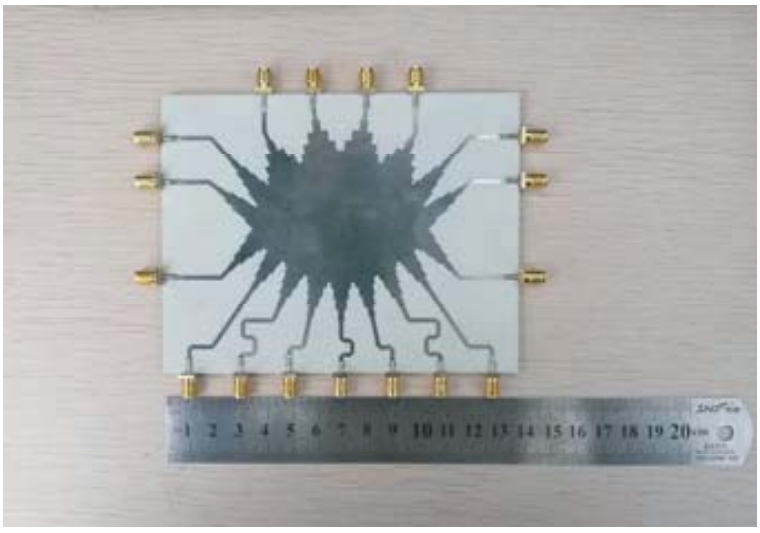

Figure 2. Photograph of the fabricated Rotman lens.

different flare angles θ is simulated with the electromagnetic simulator ANSYS HFSS 15. As shown in Table 3, it is clear that when the value of θ increases from 12° to 36°, both the bandwidth (VSWR < 1.5) of the beam ports decreases and the insertion loss of beam ports at 10 GHz decrease. Compared to the traditional Rotman lens, the Chebyshev impedance transformer can realize good match between the lens body and feed lines with shorter length. The smaller insertion loss can be obtained attributed to

lower path loss of the Chebyshev impedance transformers.

Both the Chebyshev impedance transformers and linear tapered transition ($\theta = 12°$) can realize good match between the lens body and feed lines in the X band. However, it is noted that the Chebyshev impedance transformer has smaller size and lower insertion loss than the linear tapered transition ($\theta = 12°$). It can be seen that the Chebyshev impedance transformers lead to a size reduction of about 56% for the Rotman lens.

3. EXPERIMENTAL RESULTS AND DISCUSSION

An X-band 4×7 Rotman lens using Chebyshev impedance transformers is designed and fabricated. A photograph of the prototype is shown in Fig. 2. The prototype is tested for the purpose of demonstration. The measured and simulated results are given and discussed in detail.

Figure 3(a) shows the measured and simulated return losses of beam ports B1–B4, which are in

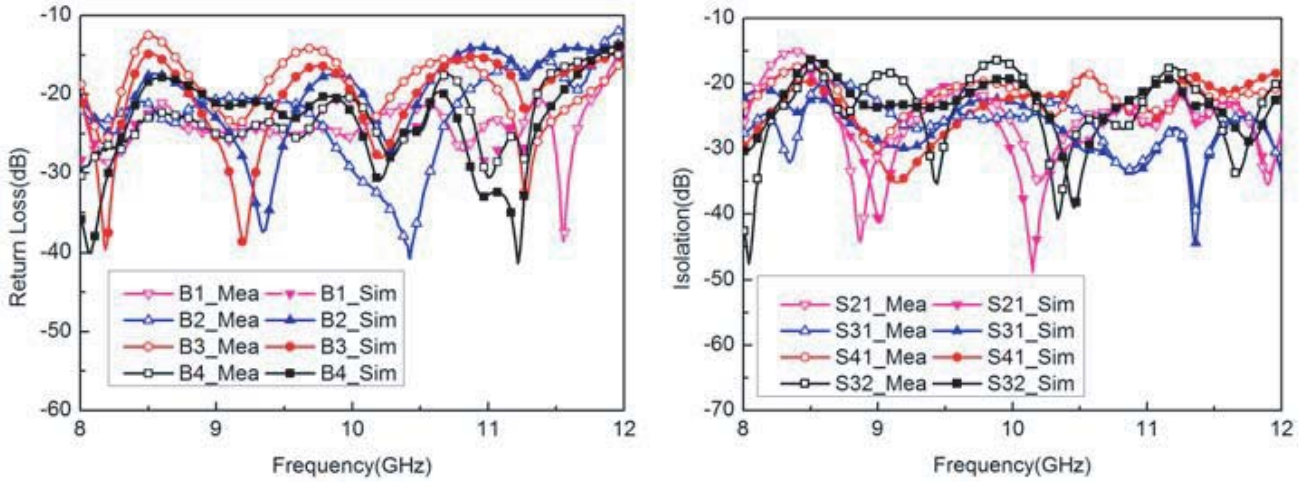

Figure 3. (a) Return losses of beam ports. (b) Isolations between beam ports.

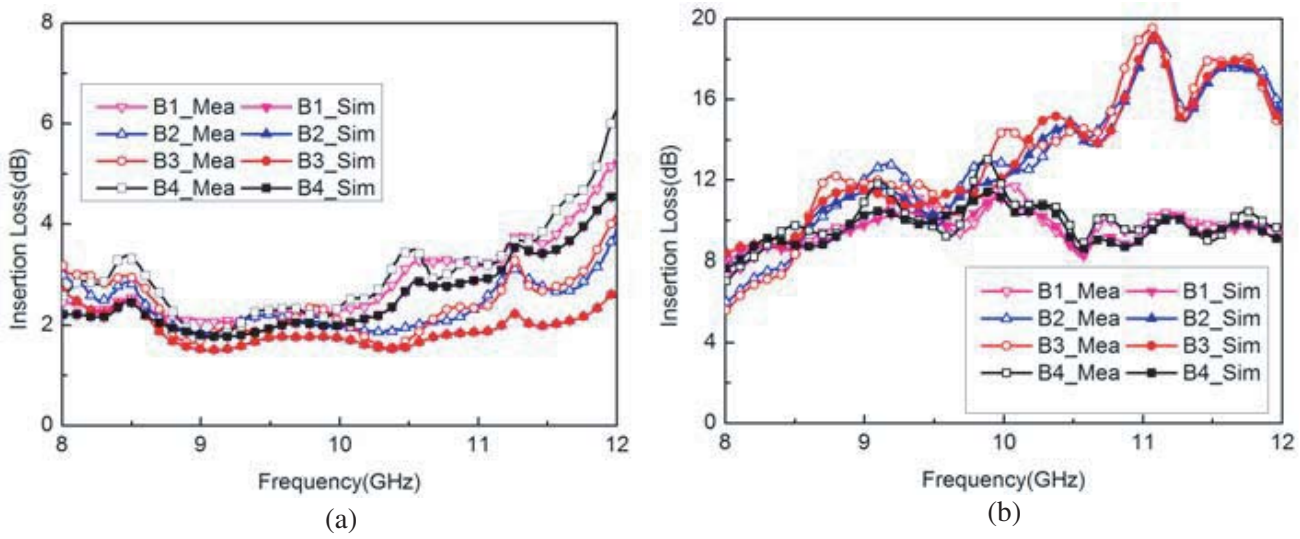

Figure 4. (a) Total insertion losses from beam ports to array ports. (b) Total insertion loss from the beam ports to dummy ports.

good agreement. The proposed Rotman lens shows a return loss better than 15 dB throughout the bandwidth from 8 to 12 GHz. Fig. 3(b) shows the isolations between beam ports S21, S31, S41, and S32. The isolations are under −15 dB over the frequency band from 8 to 12 GHz. Fig. 4(a) shows the measured and simulated total insertion losses from beam ports B1–B4 to the array ports. Fig. 4(b) shows the measured and simulated insertion losses from beam port to dummy ports. The proposed Rotman lens has low insertion losses at 10 GHz.

Figure 5 shows the measured amplitude distribution and phase distribution across array ports of the proposed Rotman lens at 10 GHz. The proposed Rotman lens exhibits taper amplitude distributions and equal phase differences across the array ports, which is beneficial to reducing the sidelobe level of the forming beams.

Array factor is an important parameter of the Rotman lens, which can provides beam direction, angle, and level of sidelobes. Through the amplitude and phase data, the array pattern can be calculated by the method in [4] at 10 GHz center frequency. The simulated array factors of the traditional Rotman lens with different flare angles when B2 is active are shown in Fig. 6(a). The array factor results of the

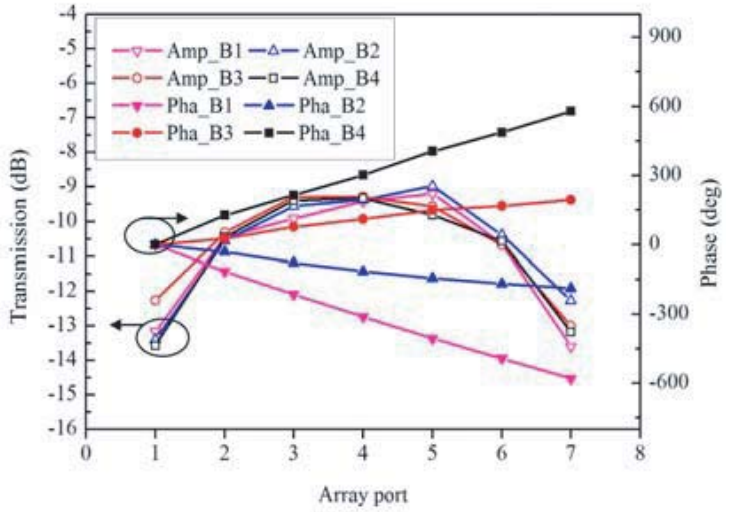

Figure 5. Measured amplitude distribution and phase distribution across array ports.

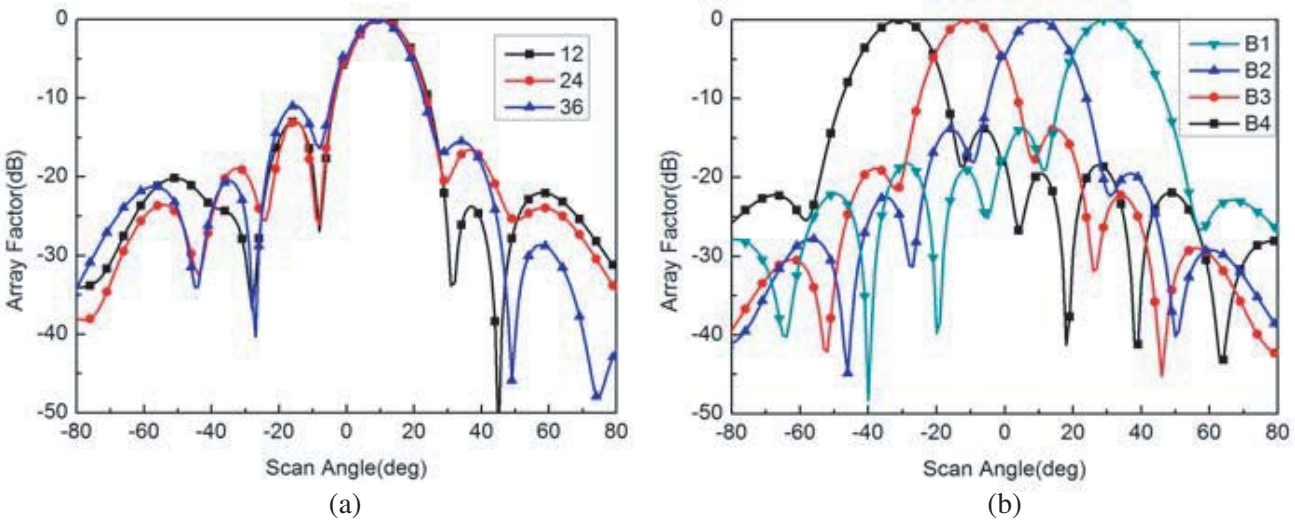

Figure 6. (a) Array factors of the traditional Rotman lens with different flare angle when B2 is active. (b) The array factor results of the proposed Rotman lens.

proposed Rotman lens are shown in Fig. 6(b). Compared to a traditional Rotman lens, the sidelobe level of the proposed Rotman lens is smaller. The result shows that the proposed Rotman lens can realize electronically controlled beam scanning from $-30°$ to $30°$ in $20°$ increments.

4. CONCLUSION

In this paper, a compact microstrip Rotman lens is presented. The size reduction about 56% for the Rotman lens is achieved by using a Chebyshev impedance transformer to replace the traditional linear tapered transition. The microstrip transitions between the lens body and Chebyshev impedance transformer are used to realize real resistances of the lens body apertures. An X-band prototype is fabricated and measured to validate its performance experimentally. The return loss of better than 15 dB throughout the bandwidth from 8 to 12 GHz and an insertion loss improvement at 10 GHz are obtained. Consequently, the advantages of simple structure, easy processing, compact size, high efficiency make it a good candidate for multi-beam antenna systems.

REFERENCES

1. Sinha, Nirmalendu Bikas, R.-N. Bera, and M. Mitra, "Digital array MIMO radar and its performance analysis," *Progress In Electromagnetics Research C*, Vol. 4, 25–41, 2008.
2. Hong, T., M.-Z. Song, and X.-Y. Sun, "Design of a sparse antenna array for communication and direction finding applications based on the Chinese remainder theorem," *Progress In Electromagnetics Research*, Vol. 98, 119–136, 2009.
3. Rotman, W. and R. F. Turner, "Wide-angle microwave lens for line source applications," *IEEE Transactions on Antennas Propagation*, Vol. 11, No. 6, 623–632, Nov. 1963.
4. Attaran, A., R. Rashidzadeh, and A. Kouki, "60 GHz low phase error Rotman lens combined with wideband microstrip antenna array using LTCC technology," *IEEE Transactions on Antennas and Propagation*, Vol. 64, No. 12, 5172–5180, Dec. 2016.
5. Attaran, A. and S. Chowdhury, "Fabrication of a 77 GHz Rotman lens on a high resistivity silicon wafer using lift-off process," *International Journal of Antennas and Propagation*, 1–9, article ID: 471935, 2014.
6. Attaran, A., R. Rashidzadeh, and R. Muscedere, "Rotman lens combined with wide bandwidth antenna array for 60 GHz RFID applications," *Int. J. Microw. Wireless Technol.*, Vol. 9, No. 1, 1–7, Aug. 2015.
7. Cheng, Y. J., et al., "Substrate integrated waveguide (SIW) Rotman lens and its Ka-band multibeam array antenna applications," *IEEE Transactions on Antennas and Propagation*, Vol. 56, No. 8, 2504–2513, Aug. 2008.
8. Lee, W., J. Kim, C. S. Cho, and Y. J. Yoon, "Beamforming lens antenna on a high resistivity silicon wafer for 60 GHz WPAN," *IEEE Transactions on Antennas and Propagation*, Vol. 58, No. 3, 706–713, Dec. 2010.
9. Vo Dai, T. K., T. Nguyen, and O. Kilic, "A compact microstrip Rotman lens design," *Radio Science Meeting*, 1–2, United States National Committee of URSI National, Boulder, USA, 2017.
10. Tekkouk, K., M. Ettorre, L. Le Coq, and R. Sauleau, "Multi-beam SIW slotted waveguide antenna system fed by a compact dual-layer Rotman lens," *IEEE Transactions on Antennas and Propagation*, Vol. 64, No. 2, 504–514, Nov. 2016.
11. Young, L., "Stepped-impedance transformers and filter prototypes," *IRE Trans. Microwave Theory Tech.*, Vol. 10, No. 5, 339–359, Sep. 1962.